Pergamon

Int. J. Non-Linear Mechanics, Vol. 32, No. 1, pp. 187–199, 1997

0020–7462/97 $17.00 + 0.00

S0020-7462(96)00042-X

EXTRUSION OF POWER-LAW SHEAR-THINNING FLUIDS WITH SMALL EXPONENT

S. J. Chapman,* A. D. Fitt† and C. P. Please†

*Mathematical Institute, University of Oxford, 24–29 St Giles, Oxford OX1 3LB, U.K.
†Faculty of Mathematical Studies, University of Southampton, Southampton SO17 1BJ, U.K.

(*Received* 5 *July* 1994)

Abstract—The slow flow of power-law shear-thinning fluids during extrusion is considered for materials where the exponent is asymptotically close to zero. Such flows arise in a number of practical industrial problems and give rise to some unexpected effects. Three different regions of extrusion flow are examined. First, some simple results for unidirectional flow in a one-dimensional channel are considered. Secondly, the region near to the die exit is then considered, and it is noted that an exponential asymptotic approach may be used to completely solve the problem of slow flow in a wedge with a sink at the vertex. Finally, the ram region of the extruder is considered and a detailed analysis is given of flow in a corner driven by the movement of one of the walls. Copyright © 1996 Elsevier Science Ltd.

Keywords: power-law fluids, shear thinning

1. INTRODUCTION

For many years the process of extrusion has been important in a great number of industrial processes. These range from the manufacture of propellants for tank guns and the drawing of optical fibres to the production of beefburgers and potato fries. One of the most common uses for extrusion is for forming ceramics. Many everyday items, such as pipes, conduits and building components, are manufactured in this way, and the process is also used to fashion extruded industrial chemical products.

Much literature is available concerning general aspects of the process of extrusion. A good survey of the extrusion mechanics of paste mixtures is given by Benbow *et al.* [1], whilst qualitative guidelines on the design of a variety of different sorts of extruders may be found in Waye [2]. One of the consequences of the nature of extrusion products is that most of the materials concerned in such processes are non-linear, and the Newtonian assumption that the stress depends linearly upon the strain rate does not produce acceptable results. The material non-linearity leads to some interesting and well-documented effects such as die-swell, and to model extrusion phenomena accurately it is essential that realistic rheological laws are employed.

Many models that attempt to describe the material non-linearities found in real materials have been proposed. In the Bingham fluid model (which has proved especially useful in soil mechanics) it is assumed that, whilst during flow the material is Newtonian, there is a complete absence of flow until some critical "yield stress" is reached. Another alternative is to assume that the relationship between the stress and the strain rate is given by a power law, whilst the Herschel–Bulkley model supplements the power-law relationship with a yield stress criterion. In this study we shall assume that the fluids under consideration have zero yield stress (experiments have shown that, although in reality a yield stress is present, it may be regarded as negligible) but exhibit a power-law stress/strain rate curve. In particular, we shall be concerned with materials that are *shear-thinning*, so that the exponent (labelled ε) in the power law is less than unity. Typically such fluids flow more easily under shear as some internal structure in the material is broken down.

A large variety of shear-thinning fluids are in common use; some examples are furnished by cosmetic cold cream ($\varepsilon \approx 0.1$–0.4), chocolate ($\varepsilon \approx 0.4$), toothpaste ($\varepsilon \approx 0.3$), ice cream (ε strongly dependent on temperature), molten polymers ($\varepsilon \approx 0.6$) and photographic chemicals [3]. In some circumstances multiphase fluids may also be satisfactorily modelled as

Owing to the complications introduced by the non-linearities of such materials, many authors have resorted to flow codes in an attempt to understand the properties of extrusion processes. Flow code calculations for flow through a square-entry die were reported by Zhang *et al* [5] who were able to identify "dead" regions in the flow where the fluid was, to all intents and purposes, stationary In most extrusion problems, such regions are undesirable as they may lead to a variety of non-uniformities in the extruded product. The consequences of dead regions may be particularly severe in cases where the material being extruded is a food product, in which a long residence time of material in the dead region may lead to bacterial contamination and other potential health risks.

The current study was motivated in part by a particular extrusion problem. A clay suspension is forced by a moving ram through a plate punctured with holes, and the resulting ceramic honeycomb forms an essential component in automobile catalytic convertors. The clay suspension used in this process has the interesting property that the exponent ε is typically less than 1/10, and, under some circumstances, may be as little as 0.03 The focus of the current study is to exploit the smallness of this exponent; the results are also applicable to a number of lubricating greases that also possess small shear-thinning exponents. In all of the industrial processes where such materials are used, the flow is slow enough for inertia to be unimportant, and accordingly we ignore all inertial terms in the equations of motion

Our aim is to examine three regions of extrusion flow; these regions are shown schematically in Fig. 1. Away from the ram or the die exit, the flow is approximately unidirectional, and accordingly in Section 2 we briefly consider simple one-dimensional channel flows, showing that when ε is small the flow is very sensitive to changes in geometry or material properties. Next, the flow near the exit of the die is considered. Although experimental and flow-code studies of such flows are clearly important, it is also crucial that the basic fluid mechanical properties of such flows are determined. In particular, a theoretical understanding of the flow into a wedge with a sink at the vertex is required. This geometry is particularly amenable to theoretical consideration as it evidently possesses no innate length scale. This allows the governing partial differential equations to be reduced to ordinary differential equations using a similarity transformation. In Section 3 the general slow-flow similarity problem is considered, whilst in Section 4 the particular case of wedge flow is highlighted. Wedge flows of power-law shear-thinning fluids were studied numerically by Mansutti and Rajagopal [6]. They considered a range of power-law exponents and solved the resulting ordinary differential equations numerically. For values of the shear-thinning exponent that were close to zero, they found that narrow boundary layers existed near the wedge walls. Such boundary layers are a consequence of the non-linearity of the stress–strain law that has been assumed As the value of the shear-thinning exponent decreased towards zero standard numerical methods proved inadequate and special schemes that do not explicitly introduce derivatives of the unknown functions were required. These were discussed in Mansutti and Pontrelli [7]. In Section 4 it is noted that, in contrast to the purely numerical approach described above, for small values of ε the whole problem may be solved in closed form using matched asymptotic expansions. An intricate boundary layer structure is revealed.

Finally, the flow near to the extrusion ram is considered. This problem may be tackled by considering the flow in a corner driven by the movement of one wall parallel to itself.

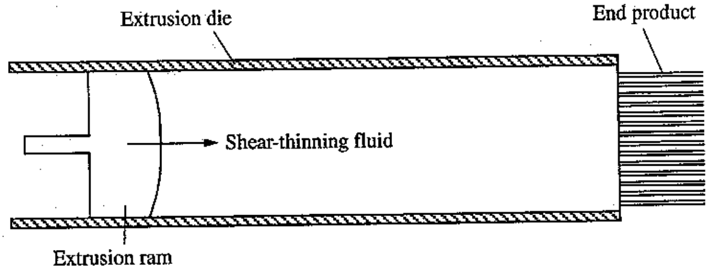

2. CHANNEL FLOW PROBLEMS

First, we briefly consider the flow in the extruder away from the ends of the device. To illustrate some of the effects that may appear when ε is small, we highlight some of the properties of one-dimensional shear-thinning flow in a channel. The fluid is assumed to occupy the region $-b \leqslant x \leqslant b$ and a velocity of the form $\mathbf{q} = (0, v(x), 0)^T$ is sought. The stress tensor is given by

$$T_{ij} = -p\delta_{ij} + \tau_{ij}$$

where

$$\tau_{ij} = \mu K \dot{\gamma}_{ij}, \quad K = |(\dot{\gamma}_{kl}\dot{\gamma}_{kl})|^{\frac{\varepsilon-1}{2}}.$$

The equations of motion thus become

$$-p_x = 0, \quad (\mu K v_x)_x - p_y = 0.$$

Hence p is a function of y only and p_y is a constant, which we take to be $P > 0$ so that the flow is in the negative y-direction. Imposing the no-slip boundary condition at the walls, it is easily shown that the velocity for $x \geqslant 0$ is given by

$$v = A[x^{1+\frac{1}{\varepsilon}} - b^{1+\frac{1}{\varepsilon}}]$$

where

$$A = \left(\frac{P}{2\mu}\right)^{\frac{1}{\varepsilon}}\left(\frac{\varepsilon}{1+\varepsilon}\right)2^{\frac{1+\varepsilon}{2\varepsilon}}.$$

The mass flow M associated with this flow is given by

$$M = -2\rho A b^{2+\frac{1}{\varepsilon}} \frac{1+\varepsilon}{1+2\varepsilon}.$$

This flow displays some interesting properties when ε is small. First, we note that if a pressure gradient P is imposed where when $Pb/\sqrt{2}\mu = 1$ then the mass flow is $O(1)$. In contrast, we find that if P is slightly smaller than this value the mass flow is very small and the fluid moves only very slowly, whilst if P is slightly greater than this value the mass flow is large and so are the corresponding fluid velocities. The details of the flow are thus extremely sensitive to changes in the pressure gradient. By the same token, an $O(\varepsilon)$ change in b, the channel semi-width, leads to an $O(1)$ change in the mass flow. The important conclusion as far as extrusion is concerned is that even minor changes in the flow conditions may have an important influence on the gross flow properties.

A range of similar Couette flow problems may also be examined by solving the equations exactly; it is worth remarking that, in these simple cases, the slow flow solutions generated are actually solutions to the full Navier–Stokes equations as the inertia terms are identically zero.

3 MATHEMATICAL FORMULATION OF THE SLOW FLOW PROBLEM

For wedge and corner flows we consider a cylindrical coordinate system (r, θ) centred at the wedge or corner apex and assume that $\mathbf{q} = u\mathbf{e}_r + v\mathbf{e}_\theta$ where $\mathbf{e}_r$ and $\mathbf{e}_\theta$ are unit vectors r and θ directions, respectively. We assume that the flow is slow so that the inertial terms in the equations may be ignored. As discussed previously, the equations of motion are given by

$$\operatorname{div} T = 0, \quad \operatorname{div} \mathbf{q} = 0$$

with

$$T_{ij} = -p\delta_{ij} + \tau_{ij}$$

and

In component form, this gives

$$-p_r + \mu K\left(u_{rr} + \frac{u_r}{r} + \frac{u_{\theta\theta}}{r^2} - 2\frac{v_\theta}{r^2} - \frac{u}{r^2}\right) + 2\mu K_r u_r + \mu K_\theta\left(\frac{v_r}{r} + \frac{u_\theta}{r^2} - \frac{v}{r^2}\right) = 0,$$

$$-\frac{p_\theta}{r} + \mu K\left(v_{rr} + \frac{v_r}{r} + \frac{v_{\theta\theta}}{r^2} + 2\frac{u_\theta}{r^2} - \frac{v}{r^2}\right) + \mu K_r\left(v_r - \frac{v}{r} + \frac{u_\theta}{r}\right) - 2\mu K_\theta \frac{u_r}{r} = 0,$$

$$(ru)_r + v_\theta = 0,$$

where K is given by

$$K = \left[\frac{u^2}{r^2} + \frac{v^2}{2r^2} + \frac{u_\theta^2}{2r^2} + \frac{v_r^2}{2} + \frac{v_r u_\theta}{r} - \frac{v u_\theta}{r^2} + u_r^2 + \frac{2u v_\theta}{r^2} - \frac{v v_r}{r} + \frac{v_\theta^2}{r^2}\right]^{\frac{\varepsilon-1}{2}}.$$

Because there is no length scale present, we seek solutions of the equations where the stream function is given by

$$\psi = r^\lambda F(\theta) \tag{1}$$

so that

$$u = r^{\lambda-1}F'(\theta), \quad v = -\lambda r^{\lambda-1}F(\theta).$$

Defining $m = (\varepsilon - 1)/2$ (the notation used in [6]) we have

$$K = \frac{\Phi^m}{2^{2m} r^{2m(2-\lambda)}}$$

where

4λ(2−λ)

$$\Phi = (8(1-\lambda)^2 F'^2 + 2F''^2 + 2\lambda^2(2-\lambda)^2 F^2 + 2\lambda(3-\lambda)FF''),$$

and the equations of motion are

$$-p_r + \frac{\mu r^k}{2^{2m}}[\Phi^m(F''' + \lambda^2 F') + 4m(\lambda-2)(\lambda-1)F'\Phi^m + (\Phi^m)'(\lambda(2-\lambda)F + F'')] = 0,$$

$$-\frac{p_\theta}{r} + \frac{\mu r^k}{2^{2m}}[\Phi^m(2-\lambda)(F'' + \lambda^2 F) + 2m(\lambda-2)\Phi^m(F'' + \lambda(2-\lambda)F) - 2(\lambda-1)F'(\Phi^m)'] = 0$$

where $k = \lambda - 3 + 2\lambda m - 4m$.

Elimination of the pressure by cross-differentiation gives

$$\begin{aligned}
&\Phi^m(F'''' + (\lambda^2 + (\lambda-2)[(\lambda-2)(1-4m^2) + 4m(\lambda-1)])F'' \\
&\quad + \lambda(\lambda-2)(k+1)(\lambda + 2m(\lambda-2))F) \\
&\quad + (\Phi^m)'(2F''' + (2\lambda + (\lambda-1)(\lambda-2)(8m+2))F') \\
&\quad + (\Phi^m)''(F'' + \lambda(2-\lambda)F) = 0
\end{aligned} \tag{2}$$

Equation (2) must be solved subject to suitable no-slip and symmetry conditions. In its most general form, this problem must be solved numerically; however we wish to focus our attention on particular values of λ.

4 JEFFREY–HAMEL FLOW IN A WEDGE

The die exits of extrusion devices used to make parts for catalytic converters typically contain hundreds of holes. Frequently, during extrusion, dead regions may form that divert the flow preferentially through some holes, whilst restricting the flow through others. This restriction may lead to hole blockage. The severity of the product design constraints means that, under some circumstances, production may have to be interrupted if as few as four holes are blocked. Experimental evidence has shown that such choking tends to occur more at low flow rates, suggesting a linkage between choking and dead zones. It is also known that the flow is sensitive to hole diameter and surface roughness. In order to be able to

Viscous flow in a wedge with a source or sink at the vertex is a classical fluid mechanics problem and has been studied in many different forms and for many different types of fluid. For a linear viscous fluid ("Jeffrey–Hamel flow") it has long been known that there is a critical wedge angle beyond which pure inflow or outflow solutions are impossible and regions of reversed flow are necessarily present [8] This is essentially a consequence of the inertial terms in the equations, and it may easily be shown that for non-inertial flow no such maximum wedge angle exists. To analyse purely radial symmetrical shear-thinning flow in a wedge we set $\lambda = 0$ in (1). Assuming that the wedge occupies the region $-\alpha \leqslant \theta \leqslant \alpha$ and that the total volume flux is given by q so that

$$\int_{-\alpha}^{\alpha} ru \, \mathrm{d}\theta = 2\int_{0}^{\alpha} F(\theta)\, \mathrm{d}\theta = q,$$

we are required to solve the ordinary differential equation

$$\Phi^m[F'''' + (4 + 8m - 16m^2)F''] + (\Phi^m)'[2F''' + (4 + 16m)F'](\Phi^m)''F' = 0$$

with boundary conditions

$$F(0) = 0, \quad F(\alpha) = -\frac{q}{2}, \quad F'(\alpha) = 0, \quad F''(0) = 0.$$

The differential equation may be rewritten

$$\begin{aligned} F''''(4F'^2 + F''^2)(4F'^2 + \varepsilon F''^2) + (\varepsilon - 1)F''F'''(32\varepsilon F'^3 + \varepsilon F''^2 F''' \\ + 16\varepsilon F F''^2 + 12F'^2 F''' - 16F'F''^2 + 32F'^3) \\ + 4F''(-2F''^4 + 16\varepsilon^2 F'^4 + 4\varepsilon^2 F'^2 F''^2 - \varepsilon^2 F''^4 + 4\varepsilon F''^4 + 4F''^2 F'^2) = 0 \end{aligned}$$

and considerable simplifications may now be made by first setting $F' = -e^G$ (this gives solutions corresponding to flow towards the vertex; for the outflow problem the negative sign is merely omitted) and then further substituting $G' = f$. The problem then reduces to

$$\begin{aligned} (f^2 + 4)(4 + \varepsilon f^2)f'' - (1 - \varepsilon)(12 + \varepsilon f^2)f(f')^2 \\ + (4 + f^2)ff'[4(1 + 2\varepsilon^2) + \varepsilon(1 + 2\varepsilon)f^2] + \varepsilon^2(4 + f^2)^3 f = 0 \qquad (3) \end{aligned}$$

with boundary conditions $f(0) = 0$, and $f = o((\theta - \alpha)^{-1})$ as $\theta \to \alpha$. The latter condition ensures that $G \to -\infty$ as $\theta \to \alpha$; f may also be $O((\theta - \alpha)^{-1})$ so long as the constant of proportionality is strictly positive.

The solution of the problem described above proceeds via the method of matched asymptotic expansions [9] by considering the limit of interest in the current, study, namely $\varepsilon \to 0$ The asymptotic analysis reveals that various terms of (3) are important in various different regions in the flow In the interior of the wedge there is an "outer" region, whilst adjacent to the wall $\theta = \alpha$ there is a narrow boundary layer. This boundary layer has a subtle structure with three separate regions of behaviour. The structure of the solution in these "inner–inner", "inner" and "transition" layers and the required matching may be completely determined in closed form; for details the reader is referred to Brewster *et al.* [10]. Notwithstanding these somewhat technical details, most of the flow takes place in the outer region and therefore much of the behaviour may be gleaned by considering this region only

In the outer region where both θ and f are order one we may determine the lowest-order behaviour of the solution by setting $\varepsilon = 0$ in (3). This gives

$$(4 + f^2)f'' - 3f(f')^2 + (4 + f^2)ff' = 0$$

which possesses a first integral

where A is a constant, which physical arguments show must be greater than $\sqrt{2}$. This may be further integrated to yield an implicit solution for $f(\theta)$ in the form

$$\theta = \tan^{-1}w - \frac{A}{\sqrt{A^2-2}}\tan^{-1}\left(\sqrt{\frac{A+\sqrt{2}}{A-\sqrt{2}}}\,w\right)$$

where

$$w = \tanh\left(\frac{1}{2}\sinh^{-1}\frac{f}{2}\right)$$

This solution does not diverge in the correct manner as $\theta \to \alpha$, which is why there is a boundary layer structure near to the wedge walls. Nevertheless, in order to make $f(\theta)$ large as $\theta \to \alpha$, we require that A satisfies the equation

$$\alpha = \frac{A}{\sqrt{A^2-2}}\tan^{-1}\left(\sqrt{\frac{A+\sqrt{2}}{A-\sqrt{2}}}\right) - \frac{\pi}{4},$$

thereby determining the wedge semi-angle α in terms of A.

By examining the original equations, the physical significance of A is easily determined; it transpires that A is the pressure gradient in the flow. We further find that the leading-order pressure gradient simply determines the order of magnitude of the mass flux and the actual value of q is determined by the next order correction to the pressure gradient. We note that, for a prescribed wedge semi-angle α, A is effectively determined. If the applied pressure gradient P is *not* equal to A, then the mass flux is no longer order one; in fact if $P < A$ the mass flux is exponentially small, whilst if $P > A$ the mass flux is exponentially large. This confirms the extreme sensitivity of the flow to pressure gradient and geometry.

Comparisons between the asymptotic solution and the numerical results of [7] show excellent agreement; for small values of ε the differences are negligible. Furthermore, the results of the asymptotic analysis remain satisfactory even for values of the shear-thinning exponent up to about 0.3 Figure 2 shows a typical velocity profile $\exp(G(\theta))$ $(= -u/r)$, computed with $A = 1.9121$ (corresponding to a wedge semi-angle of 1 radian) and $\varepsilon = 0.12$ $(m = -0.44)$. The value at $\theta = 0$ predicted by the asymptotic solution is 1.396, which agrees well with the value of 1.393 from the numerical calculations of [7].

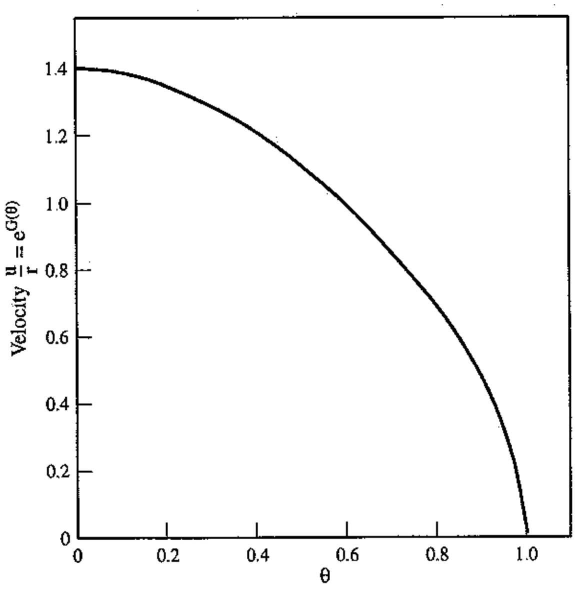

5 DRIVEN FLOW IN A CORNER

Finally, we examine the flow near to the extrusion ram. Locally, it is evident that the flow is equivalent to that produced by driven flow in a corner, the flow being produced by the movement of one wall parallel to itself. Many rams are not straight-faced, so the analysis below is carried out for a general corner angle, labelled α. For simplicity we assume that the wall $\theta = \alpha$ is fixed and that the wall $\theta = 0$ moves with a (constant) velocity $U\mathbf{e}_r$. For the ram (Fig. 1), U would be negative. In contrast to the previous section, we consider the case where there is no net mass flow into the corner $r = 0$ of the vertex.

The physical problem described above suggests seeking a solution to the equations of motion presented in Section 3 with $\lambda = 1$ and boundary conditions

$$F(0) = F(\alpha) = 0, \quad F'(0) = 1, \quad F'(\alpha) = 0.$$

For simplicity, U has been scaled out of the problem; for values of U not equal to 1, a solution may be generated by simply multiplying F by U. Because the strain rate $\dot{\gamma}$ changes sign in this problem, a little extra care is required to ensure that the viscosity is interpreted correctly. Substituting $\lambda = 1$ in the equations of Section 3 gives

$$-p_r + \frac{\mu r^{-2-2m}}{2^{2m}}[|\Phi|^m(F'' + F)]' = 0,$$

$$-\frac{p_\theta}{r} + \frac{\mu r^{-2-2m}}{2^{2m}}[(1-2m)|\Phi|^m(F'' + F)] = 0.$$

Elimination of the pressure terms gives

$$[|\Phi|^m(F'' + F)]'' + (1 - 4m^2)|\Phi|^m(F'' + F) = 0,$$

and this may be solved by defining $G(\theta) = |\Phi|^m(F'' + F)$ so that G satisfies the equation

$$G'' + (1 - 4m^2)G = 0 \tag{4}$$

Since in the current study we are interested specifically in shear-thinning fluids with $0 < \varepsilon \leqslant 1$, the parameter $1 - 4m^2$ is never negative; we remark in passing that for shear-thickening fluids with $\varepsilon > 2$, equation (4) will possess exponential solutions. Defining $\nu = \sqrt{1 - 4m^2} = \sqrt{2\varepsilon - \varepsilon^2}$ for convenience, we find that

$$G = A\cos(\nu\theta + B)$$

where A and B are arbitrary constants. Using the definition of $G(\theta)$, we find that F satisfies

$$F'' + F = q(\theta)$$

where

$$q(\theta) = A\cos(\nu\theta + B)|A\cos(\nu\theta + B)|^{\frac{1}{\varepsilon}-1}$$

The solution to this equation is given by

$$F = \sin\theta\left[\int_C^\theta q(t)\cos t\,\mathrm{d}t\right] - \cos\theta\left[\int_D^\theta q(t)\sin t\,\mathrm{d}t\right] \tag{5}$$

and the boundary conditions must now be imposed. Two of the boundary conditions may be satisfied by taking $C = \alpha$ and $D = 0$; the remaining two conditions then require that A and B be chosen so that

$$\int_0^\alpha q(t)\cos t\,\mathrm{d}t = -1 \tag{6}$$

$$\int_0^\alpha q(t)\sin t\,\mathrm{d}t = 0. \tag{7}$$

Before considering the case of asymptotically small ε, we note that, when the flow is Newtonian, we have $\varepsilon = 1$, $\nu = 1$ and $q(t) = A\cos(t + B)$. Conditions (6) and (7) give

$$\left[\quad \sin^2\alpha \quad \right] \qquad -2\sin^2\alpha$$

and the stream function is therefore given by

$$\psi = rF(\theta) = \frac{r}{\alpha^2 - \sin^2\alpha}\left[\alpha(\alpha-\theta)\sin\theta + \theta\sin\alpha\sin(\theta-\alpha)\right].$$

It is easily confirmed that this is the correct solution for the Newtonian case $\varepsilon = 1$.

When ε is small, it is possible to proceed using matched asymptotic expansions as in the previous section. In the current case, however, it is simpler to determine A and B directly from (6) and (7). To do this, we note that if (7) is to be enforced for arbitrary α, then there must be a point in the interior of the interval $[0, \pi/2]$ where $\nu\theta + B$ takes the value $\pi/2$ so that the cosine term in $q(t)$ changes sign. This allows (7) to be written

$$\int_0^{\frac{\pi/2-B}{\nu}} (\cos(\nu t + B))^{\frac{1}{\varepsilon}} \sin t \,\mathrm{d}t - \int_{\frac{\pi/2-B}{\nu}}^{\alpha} (-\cos(\nu t + B))^{\frac{1}{\varepsilon}} \sin t\,\mathrm{d}t = 0.$$

Denoting the integrals in the expression above by I_1 and I_2, respectively, we consider the limit $\varepsilon \to 0$, using Laplace's method to determine asymptotic expansions for I_1 and I_2.

Considering I_1 first, it is convenient to write the integral in the form

$$I_1 = \int_0^{\frac{\pi/2-B}{\nu}} \exp\left(\frac{h(t)}{\varepsilon}\right) g(t)\,\mathrm{d}t$$

where $h(t) = \log\cos(\nu t + B)$, $g(t) = \sin t$. In the region of integration, $h(t)$ takes its maximum value at the left-hand end-point $t = 0$. For small ε, the integral will therefore be dominated by the behaviour near to this point, other contributions being exponentially small. By expanding $g(t)$ and $h(t)$ in the normal way as Taylor series about $t = 0$ and ignoring exponentially small terms, we find that

$$I_1 \approx \frac{\varepsilon^2(\cos B)^{\frac{1}{\varepsilon}}}{\nu^2\tan^2 B}\left[1 - \frac{\varepsilon^2}{\nu^2\tan^2 B}\right]$$

As usual when using Laplace's method for integrals, the method given above may be made rigorous if required by invoking Watson's lemma [11].

If $I_1 + I_2$ is to be zero, the contribution from I_1 must balance with I_2, the contribution from the right-hand end of the interval. In the latter case, the maximum is at the point α, and Laplace's method may once again be used to estimate the integral. The requirement imposed by (7) thus becomes

$$I_1 + I_2 \approx \frac{\varepsilon^2(\cos B)^{\frac{1}{\varepsilon}}}{\nu^2\tan^2 B}\left[1 - \frac{\varepsilon^2}{\nu^2\tan^2 B}\right] + \frac{\varepsilon(-\cos(\nu\alpha + B))^{\frac{1}{\varepsilon}}}{\nu\tan(\nu\alpha + B)}\left[\sin\alpha + \frac{\varepsilon\cos\alpha}{\nu\tan(\nu\alpha + B)}\right] = 0.$$

Rearrangement of this expression reveals that

$$\cos B + \cos(\nu\alpha + B)\left[\frac{\nu\tan^2 B\left(\sin\alpha + \dfrac{\varepsilon\cos\alpha}{\nu\tan(\nu\alpha + B)}\right)}{-\varepsilon\tan(\nu\alpha + B)\left(1 - \dfrac{\varepsilon^2}{\nu^2\tan^2 B}\right)}\right]^{\varepsilon} = 0.$$

Now, by expanding for small ε, we find that to lowest order,

$$B = \frac{\pi}{2} - \frac{\alpha}{\sqrt{2}}\sqrt{\varepsilon} + \frac{\sqrt{2}\alpha}{4}\varepsilon^{3/2}\log\varepsilon + O(\varepsilon^{3/2}) \tag{8}$$

Now that B has been established asymptotically, we may also find A. Splitting the integral in (6) into two parts, (6) becomes

$$A|A|^{\frac{1}{\varepsilon}-1}(J_1 + J_2) = -1. \tag{9}$$

where

$$\int^{\frac{\pi/2-B}{\nu}} \left(\log(\cos(\nu t + B))\right) \qquad \int^{\alpha} \left(\log(-\cos(\nu t + B))\right)$$

Again, Laplace's method may be used to estimate the integrals. Accounting for the contributions from each integral, we find that

$$J_1 + J_2 \approx \frac{\varepsilon(\cos B)^{\frac{1}{\varepsilon}}}{\nu^2 \tan^2 B}\left[1 - \frac{\varepsilon^2}{\nu^2 \tan^2 B}\right] + \frac{\varepsilon(-\cos(\nu\alpha + B))^{\frac{1}{\varepsilon}}}{B \tan(\nu\alpha + B)}\left[\cos\alpha - \frac{\varepsilon \sin\alpha}{\nu \tan(\nu\alpha + B)}\right]$$

With B given by (8), we find that

$$J_1 + J_2 \approx (\cos B)^{\frac{1}{\varepsilon}} \frac{\varepsilon\alpha^2}{4}[1 - \varepsilon \log \varepsilon] - (-\cos(\nu\alpha + B))^{\frac{1}{\varepsilon}} \frac{\alpha\varepsilon}{2\cos\alpha}\left[1 + \frac{\varepsilon \log \varepsilon}{2}\right]$$

and it is convenient to rearrange (9) as

$$A|A|^{\frac{1}{\varepsilon}-1}(\cos B)^{\frac{1}{\varepsilon}}\left[\frac{\varepsilon\alpha^2(1 - \varepsilon\log\varepsilon)}{2} - \frac{(\cos \nu\alpha)^{\frac{1}{\varepsilon}}\alpha\varepsilon}{2\cos\alpha}\left(1 + \frac{\varepsilon\log\varepsilon}{2}\right)(\tan\nu\alpha \tan B - 1)^{\frac{1}{\varepsilon}}\right] = -1$$

This may now be expanded for small ε to show that A is negative and given, correct to $\sqrt{\varepsilon}$, by

$$A = -\left[\frac{\sqrt{2}}{\alpha\sqrt{\varepsilon}} + \frac{\sqrt{2\varepsilon}}{12\alpha}\left[-6\log\varepsilon + \alpha^2 - 12\log\left(\frac{\alpha^2}{4}\right)\right]\right] + O(\varepsilon^{3/2}\log\varepsilon). \tag{10}$$

The asymptotic estimates given by (8) and (10) may easily be checked by some rather tedious but basically fairly simple numerical calculations. Table 1 compares the numerical and asymptotic values of A and B for the cases $\varepsilon = 0.2$ and 0.01 for various wedge semi-angles α. Clearly the agreement between the asymptotic and exact values is excellent, and improves for small values of ε.

Now that we have found B and A asymptotically, we can also give asymptotic expression for solution (5) and the velocities u and v. It transpires that these expressions are somewhat cumbersome, and so for convenience they are given in the Appendix.

Figure 3(a) and (b) shows the streamline patterns for the Newtonian and shear-thinning ($\varepsilon = 0.1$) cases, respectively The wedge angle in both cases is given by $\alpha = 1$ and U is taken to have the value 1. In the Newtonian case the relevant values of B and A are 0.9145 and -6.123, respectively, whilst for the results shown in Fig. 3(b) we have $B = 1.3244$ (asymptotic estimate 1.3214) and $A = -5.5292$ (asymptotic estimate -5.6442). For the Newtonian case the streamline furthest from the wall has a value of 0.1631, whilst for the shear-thinning case the corresponding streamline has a value of only 0.04287. The concentration of the streamlines near to the moving wall is also clearly visible in the non-Newtonian case.

Velocity profiles for the same cases are shown in Fig. 4(a) and (b). The boundary layer structure in both velocity components and the order of magnitude decrease in v is immediately apparent for the non-Newtonian flow of Fig. (4b). For practical purposes, one quantity of interest is the mass flow into and out of the wedge, which we refer to as the "throughput" M. This is defined by the expression

$$M = \frac{1}{2}\int_0^\alpha |u| \, d\theta = \int_0^{\theta_0} u \, d\theta$$

where θ_0 is the interior value of θ where u is zero.

Table 1 Comparison of numerical and asymptotic values

	$\varepsilon = 0.2$				$\varepsilon = 0.01$			
	Numerical		Asymptotic		Numerical		Asymptotic	
α	B	A	B	A	B	A	B	A
0.1	1.5349	− 71.3826	1.5341	− 74.6110	1.5636	− 149.9450	1.5636	− 153.1527
0.2	1.4990	− 31.0775	1.4974	− 32.9295	1.5563	− 73.9090	1.5563	− 75.7980
0.3	1.4631	− 19.1131	1.4607	− 20.2522	1.5491	− 49.1862	1.5491	− 50.0183
0.5	1.3915	− 10.3964	1.3872	− 10.8759	1.5346	− 29.3361	1.5346	− 29.7267
1.0	1.2144	− 4.5925	1.2037	− 4.6007	1.4985	− 14.5955	1.4985	− 14.4684
1.5	1.0422	− 2.8964	1.0201	− 2.7691	1.4624	− 9.7053	1.4623	− 9.7171

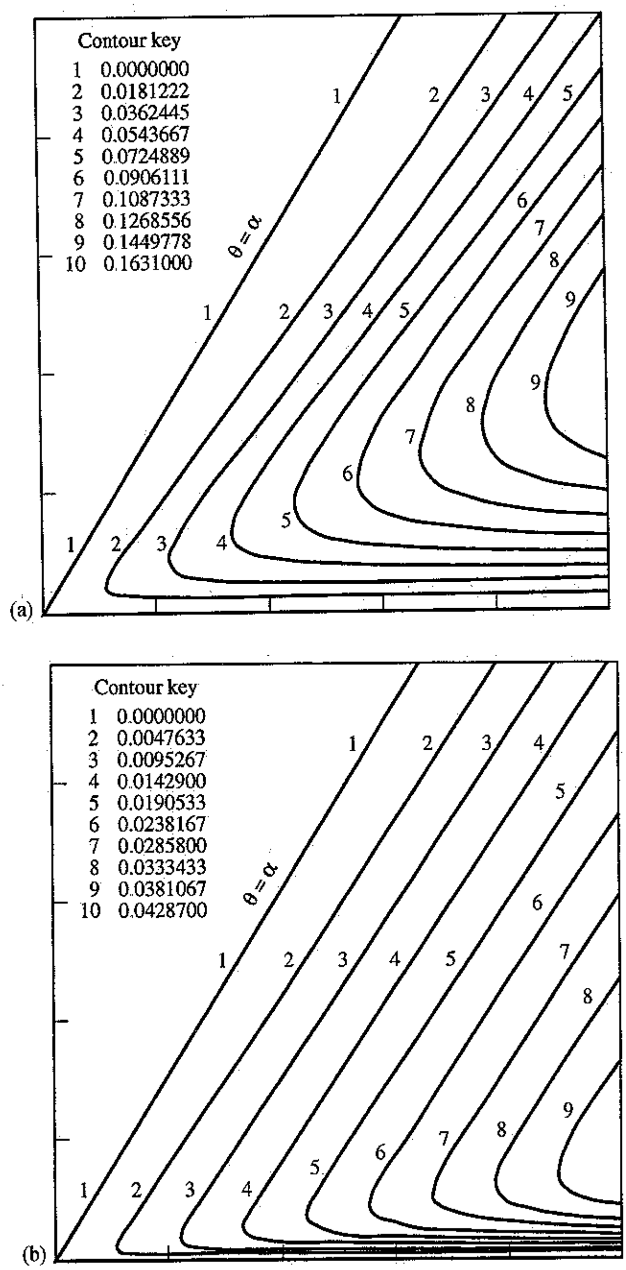

Fig. 3. (a) Streamline patterns for Newtonian flow ($\varepsilon = 1$) in a driven corner (wall velocity = 1) of angle $\alpha = 1$ radian. (b) Streamline patterns for shear-thinning flow ($\varepsilon = 0.1$) in a driven corner (wall velocity = 1) of angle $\alpha = 1$ radian.

For the Newtonian case, it is easy to confirm that θ_0 is given by the solution in $(0, \alpha)$ of the transcendental equation

$$\alpha^2 \cos\theta_0 + \sin^2\alpha(\theta_0 \sin\theta_0 - \cos\theta_0) + (\sin\alpha\cos\alpha - \alpha)(\theta_0\cos\theta_0 + \sin\theta_0) = 0 \qquad (11)$$

and that the throughput is given by

$$M = \frac{\alpha^2 \sin\theta_0 - \theta_0 \sin\alpha \sin(\alpha - \theta_0) - \alpha\theta_0 \sin\theta_0}{\alpha^2 - \sin^2\alpha}.$$

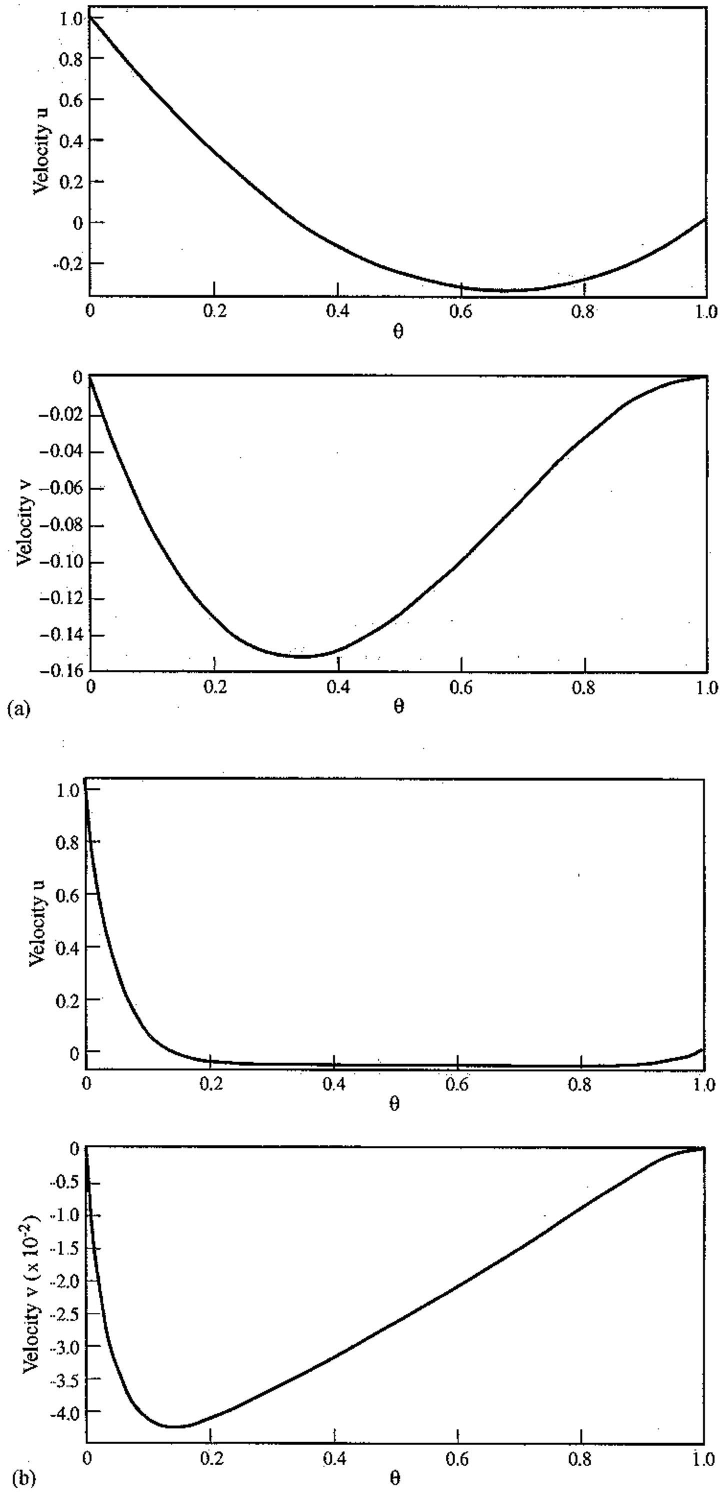

Fig. 4. (a) Velocity profiles for Newtonian flow ($\varepsilon = 1$) in a driven corner (wall velocity $= 1$) of angle $\alpha = 1$ radian. (b) Velocity profiles for shear-thinning flow ($\varepsilon = 0.1$) in a driven corner (wall velocity $= 1$) of angle $\alpha = 1$ radian.

For the shear-thinning case, a series expansion for θ_0 may be determined from the asymptotic expression for u, giving

In order to determine an asymptotic form for M, it is necessary to integrate the expression for u given in the Appendix between 0 and θ_0. Laplace's method must once again be employed to perform the integrations, and, after some rather lengthy algebra, it transpires that M is given by the particularly simple expression

$$M = \varepsilon + O(\varepsilon^2 \log \varepsilon).$$

We note that, in contrast to the Newtonian case, M does not depend to leading order on the wedge semi-angle α. This confirms that for small ε, the narrow boundary layer sees the outer flow as essentially stationary, and hence is unaffected by the value of α.

6 CONCLUSIONS AND DISCUSSION

The flow in three different regions of a ram extruder has been examined. In each region, the results clearly indicate that, when the shear-thinning exponent ε is much less than unity, the flow exhibits some interesting properties.

For one-dimensional channel flow, small changes in the geometry may have an altogether larger effect on the mass flow rate. In practical extruders the effective geometry may be changed by hole blockage and dead region formation. The analysis presented above shows that the fact that such ostensibly small blockages may seriously affect device performance should come as no surprise.

For wedge flow towards a sink, it has been shown that the wedge angle effectively determines the pressure gradient. If the pressure gradient is not "correct" then the flow rate is necessarily either exponentially small or exponentially large. In any case, wedge flows exhibit boundary layers near to the wedge walls. Such flows are completely reversible and, in contrast to inertial Newtonian flow (where there is a maximum wedge angle beyond which no pure outflow or inflow solutions exist) the boundary layers here are entirely due to the non-linearity of the fluid. In fact, when the inertial terms are retained in the equations, boundary layers of a more familiar form exist in regions near to the wall; a full study of such inertial boundary layers was carried out by Pakdemirli [12].

For driven corner flow near to the extrusion ram, it has been shown that, when the shear-thinning exponent is small, boundary layers exist near to the moving wall, and the throughput of fluid is dramatically reduced. Moreover, to leading order, the throughput is independent of the wedge angle.

Acknowledgements—This problem arose as the result of discussions at the 1993 RPI Mathematical Workshop with Industry, Troy NY, U.S.A. The authors wish to express their gratitude to Dr John Abbott of Corning Inc. for bringing the problem to our attention and providing constant and valued input to discussion of the problem.

REFERENCES

1. J. J. Benbow, E. W. Oxley and J. Bridgwater, The extrusion mechanics of pastes—the influence of paste formulation on extrusion parameters. *Chem. Engng Sci.* **42**, 2151 (1987).
2. B. E. Waye, *Introduction to Technical Ceramics*. Maclaren & Sons, London (1967).
3. S. J. Weinstein, Wave propagation in the flow of shear-thinning fluids down an incline. *AIChE J* **36**, 1873 (1990).
4. J. R. Calvert, Pressure-drop for foam flow through pipes. *Int. J. Heat Fluid Flow* **11**, 236 (1990).
5. J. Zhang, W. B. Carlson and J. S. Reed, Flow mechanics on extrusion through a square-entry die. *J. Am. Ceram. Soc.* **75**, 3011 (1992).
6. D. Mansutti and K. R. Rajagopal, Flow of a shear-thinning fluid between intersecting planes. *Int. J. Non-linear Mech.* **26**, 769 (1991).
7. D. Mansutti and G. Pontrelli, Jeffrey-Hamel flow of power-law fluids for exponent values close to the critical value. *Int. J. Non-linear Mech.* **26**, 761 (1991).
8. L. Rosenhead, *Laminar Boundary Layers*. Dover, New York (1963).
9. A. H. Nayfeh, *Perturbation Methods*. John Wiley, New York (1973).
10. M. E. Brewster, S. J. Chapman, A. D. Fitt and C. P. Please, Asymptotics of slow flow of very small exponent power-law shear-thinning fluids in a wedge. *Euro. J. Appl. Math.* **6**(6), 559 (1995).

APPENDIX

Using the notation employed in the main body of the test, we have

$$\psi = r\left[-\cos\theta\left(\int_0^\theta f(t)\sin t\,dt\right) - \sin\theta\left(\int_\theta^\alpha f(t)\cos t\,dt\right)\right],$$

$$u = \sin\theta\int_0^\theta f(t)\sin t\,dt - \cos\theta\int_\theta^\alpha f(t)\cos t\,dt$$

$$v = \cos\theta\int_0^\theta f(t)\sin t\,dt + \sin\theta\int_\theta^\alpha f(t)\cos t\,dt.$$

To determine these quantities it is therefore sufficient to determine small-ε approximations to the integrals

$$\Delta_1 = \int_0^\theta f(t)\sin t\,dt \quad \text{and} \quad \Delta_2 = \int_\theta^\alpha f(t)\cos t\,dt.$$

Noting that the sign change in $\cos(vt + B)$ occurs when $\theta = \xi$ where

$$\xi = \frac{\alpha}{2} + \frac{\varepsilon\alpha}{4}\left(\frac{1}{2} - \log\varepsilon\right) + O(\varepsilon^2\log\varepsilon)$$

we find (using Laplace's method and proceeding to second order) that for $\theta < \xi$

$$\Delta_1 = -\frac{\varepsilon^2(-A\cos B)^{\frac{1}{\varepsilon}}}{v^2\tan^2 B}\left[1 - (1 + k_1)e^{-k_1} - \frac{\varepsilon^2}{6v^2\tan^2 B}(6 - (k_1^3 + 3k_1^2 + 6k_1 + 6)e^{-k_1})\right]$$

where $k_1 = (\theta v/\varepsilon)\tan B$.

When θ exceeds ξ, the integral must be split up again and there is a new endpoint local maximum to be included. Further use of Laplace's method yields the asymptotic form for Δ_1 when $\theta > \xi$

$$\Delta_1 = -\frac{\varepsilon^2(-A\cos B)^{\frac{1}{\varepsilon}}}{v^2\tan^2 B}\left[1 - \frac{\varepsilon^2}{v^2\tan^2 B}\right] - \frac{\varepsilon(A\cos(v\theta + B))^{\frac{1}{\varepsilon}}}{v\tan(v\theta + B)}\left[\sin\theta(1 - e^{k_2}) - \frac{\varepsilon\cos\theta}{v\tan(v\theta + B)}(-1 + (1 - k_2)e^{k_2})\right]$$

where $k_2 = (-(\xi - \theta)v\tan(v\theta + B))/\varepsilon$.

A similar procedure may be used to approximate Δ_2 We find that

$$\Delta_2 = -(-A)^{\frac{1}{\varepsilon}}\left[-\frac{\varepsilon(\cos(v\theta + B))^{\frac{1}{\varepsilon}}}{v\tan(v\theta + B)}\left(\cos\theta(e^{k_3} - 1) + \frac{\varepsilon\sin\theta}{v\tan(v\theta + B)}(1 + e^{k_3}(k_3 - 1))\right)\right.$$
$$\left. + \frac{\varepsilon(-\cos(v\alpha + B))^{\frac{1}{\varepsilon}}}{v\tan(v\alpha + B)}\left(\cos\alpha(1 - e^{k_4}) + \frac{\varepsilon\sin\alpha}{v\tan(v\alpha + B)}(-1 + e^{k_4}(1 - k_4))\right)\right]$$

where $k_3 = -((\xi - \theta)v\tan(v\alpha + B))/\varepsilon$ and $k_4 = (\xi v\tan(v\alpha + B))/\varepsilon$.